

Exploring many-body localisation in open quantum systems via Wegner-Wilson flows

Shane P. Kelly,¹ Rahul Nandkishore,² and Jamir Marino^{3,*}

¹Theoretical Division, Los Alamos National Laboratory, Los Alamos, New Mexico 87545, USA

Physics and Astronomy Department, University of California Riverside, Riverside, California 92521, USA

²Department of Physics and Center for Theory of Quantum Matter, University of Colorado, Boulder, CO 80309, USA

Kavli Institute for Theoretical Physics, University of California, Santa Barbara, CA 93106-4030, USA

³Department of Physics, Harvard University, Cambridge MA 02138, USA

Department of Quantum Matter Physics, University of Geneva, 1211, Geneva, Switzerland

Kavli Institute for Theoretical Physics, University of California, Santa Barbara, CA 93106-4030, USA

(Dated: December 20, 2024)

We apply a Flow Equation method to study the problem of a many-body localised system of spinless fermions, coupled via density-density interactions to a second clean chain of fermions. In particular, we focus on the conditions for the onset of a many-body localised phase in the clean sector of our model by proximity to the dirty one. We find that a many-body localisation proximity effect in the clean component is established when the density of dirty fermions exceeds a threshold value, in a way reminiscent of recent experiments on many-body localised systems coupled to a bath. Tuning the control parameters of the model we establish thresholds for the induction of a many-body localised phase in the clean sector, using a joint set of emergent integrals of motion for the clean and dirty components as ansatz for the solution of the flow equations. Furthermore, by engineering the geometry of the inter-chain couplings, we show that the dynamics of the model can be described, on intermediate time scales, by an hamiltonian with a novel set of emergent integrals of motion.

The advent of cold gas experiments [1] has revitalised interest in the fundamental questions of quantum thermodynamics in isolated many-body systems. One of the most intriguing avenues of research is the quest for non-ergodic phases of quantum matter, which elude conventional descriptions in terms of the basic principles of statistical mechanics; examples range from fine-tuned integrable model [2, 3] to quantum scars [4], including the prominent example of ergodicity breaking by disorder: many-body localisation (MBL) [5, 6]

MBL has been the subject of intense work in the last ten years; seminal works have studied the problem both in a perturbation treatment [7–9] and with numerical methods [10–12], establishing that a localised phase which exhibits absence of diffusion on long time scales, can survive the presence of many body interactions. The interest stands from its rich phenomenology: unusual dynamical responses [13, 14], a novel pattern of quantum entanglement [15–19], the possibility to host new types of order without equilibrium counterpart [20–23], and connections to the notion of quantum integrability [15, 24–29]. In particular, MBL systems possess an extensive set of quasi-local integrals of motion, conserved by the unitary dynamics, and preventing full thermalization. Such local degrees of freedom (called localized bits or l-bits) can be constructed via a sequence of local unitary transformations starting from a free Anderson insulator, and represents a form of quantum integrability robust to perturbations. This property is at the basis of a mathematical proof of the existence of the MBL phase for one-dimensional spin lattice systems with short-range interactions [30].

MBL is nowadays investigated in experiments with cold gases [31–34] and superconducting qubits [35]. The advent of MBL in experimental platform poses naturally the question of its robustness to the coupling with an external environment [36, 37]. A bath is expected to provide sufficient energy and phase-space to facilitate the hopping in an other-

wise localised system [38–46]. On the other hand, a recent experiment [47] suggests that the clean ‘environment’ needs to reach a comparatively large density of particles with respect to the dirty MBL system in order to act as a thermodynamic environment and induce ergodic behaviour. In order to render the problem treatable, the coupling between a quantum many body system and a bath is usually assumed weak. The complementary regime, however, presents an even more interesting scenario: when the back-action on the bath is strong, and the bath and system are of comparable size, the ‘clean’ bath could localize by proximity to the dirty system – a phenomenon dubbed ‘MBL proximity effect’ [48–50].

In the last few years, renormalisation group approaches to the MBL problem have attracted increasing attention in describing the property of the localised-delocalised transition and the dynamics resulting from non-equilibrium initial states [51–56]. In this work, we study the MBL proximity effect (see Fig. 1) using the Wegner-Wilson flow equation method, a method which constructs a set of renormalisation group like equations that implement an infinitesimal stepwise diagonalisation of the many-body hamiltonian. When both the clean and dirty components of the system localize, these equations describe a transformation to an l-bit hamiltonian describing an extensive set of local conserved charges in both components. By focusing on this regime, one can make an ansatz of the l-bit hamiltonian that only includes a few relevant many-body terms. Thus, in addition to being able to study regimes of strong system-bath coupling, the flow equation method is able to access system’s sizes beyond those treatable in exact diagonalisation.

This approach allows us to identify for the MBL proximity effect a regime complementary to the one explored in the experiment in Ref. [47]: *above a certain critical density the dirty system acts effectively as a source of disorder* and induces a MBL phase into the clean component of the model.

In addition, the approach allows us also to extract results from *engineering the geometry of the system-bath coupling*. Whenever the dirty chain is smaller than the clean chain and couples every $\delta > 1$ sites, a separation of time scales emerges: on intermediate time scales, the dirty chain acts as a distribution of impurities placed every δ sites, *cutting the clean chain into a sequence of emergent conserved charges*. These integrals of motions lead to non-ergodic dynamics on intermediate time scales which cross over into thermalisation when interactions between conserved charges becomes effective and induces relaxation.

We consider a system composed of two wires of interacting spinless fermions coupled via an inter-chain density-density interaction of strength Δ_I . The Hamiltonian of the system reads

$$\begin{aligned} H &= H^c + H^d + H^I \\ H^c &= \sum_{ij} J_{ij}^c c_i^\dagger c_j + \sum_{ij} \Delta_{ij}^c n_i^c n_j^c \\ H^d &= \sum_{ij} J_{ij}^d d_i^\dagger d_j + \sum_{ij} \Delta_{ij}^d n_i^d n_j^d + \sum_k h_i^d n_i^d \\ H^I &= \sum_{ij} \Delta_{ij}^I n_i^c n_j^d \end{aligned} \quad (1)$$

where the sums run over N_s dirty sites and δN_s clean sites (with $\delta \geq 1$). The fields, h_i , are drawn from a uniform box distribution of variance W , i.e. $h_i \in [-W, W]$; for sufficiently large W , the chain of fermions, d_i , will be in the MBL phase, and will act on the clean fermionic component, c_i , as a source of disorder. Couplings in Eq. (1) contain a generic dependence on spatial indices, despite the microscopic model we study contains inhomogeneities only in the on-site fields, h_i . However, we opted for the choice of writing a general hamiltonian in (1) to emphasise that, already at the first steps of integration of the flow equations, couplings inherit an explicit spatial dependence from the disordered fields, h_i .

We study, in the following, the conditions upon which the dirty chain can induce a MBL phase in the clean component, realising an instance of the many-body localisation proximity effect. A schematic representation of the setup considered is portrayed in Fig. 1. In particular, we will consider the sensitivity of the MBL proximity effect to a broad set of control parameters: the hopping of the clean model, J^c , the inter-chain coupling, Δ^I , and the density of fermions in the MBL chain.

We plan to assess the impact of the disordered environment on the clean system using a variant of the Flow Equation (FE) method, also known as Wegner-Wilson flows (see the broad corpus of literature in [57]), tailored to treat MBL systems [58, 59]. The approach consists in iteratively diagonalising the Hamiltonian of the system in real space, for a given realisation of disorder, with a series of continuous unitary transformations.

The key idea of the FE approach is to introduce a family of unitary transformations, $U(l)$, parameterised by a 'renormalisation group' scale, l , generated by the anti-hermitian operator, $\eta(l)$, via the relation, $U(l) = T_l \exp(\int \eta(l) dl)$. The fixed

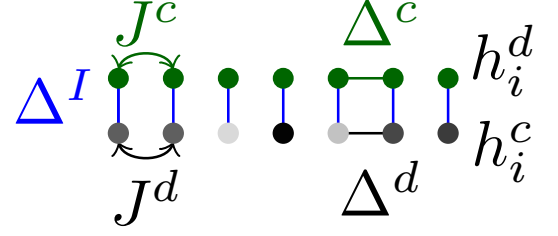


Figure 1: Sketch of the model considered in the Hamiltonian (1). The MBL sector (sites colored by various shades of grey indicating the presence of a disorder field) acts as a source of disorder to induce localisation in the clean component (green sites). The two systems are coupled site by site via inter-chain couplings (blue lines) of strength, Δ_I .

point of the FE procedure in the $l \rightarrow \infty$ limit, is a diagonal Hamiltonian with dressed couplings. Operators, $O(l)$, flow according to the equation $\frac{dO}{dl} = [\eta(l), O(l)]$. A customary choice consists in choosing $\eta(l) \equiv [H_0(l), V(l)]$, with $H_0(l)$ and $V(l)$ the diagonal and off-diagonal parts of the Hamiltonian, respectively, which guarantees vanishing off-diagonal terms at the fixed point, $l \rightarrow \infty$ [60]. Typically, the solution of an interacting quantum many-body system via the FE approach would require a broad set of variational parameters, as result of the nested hierarchies of multi-particles correlations.

However, in the case of MBL systems, a guiding insight in fixing the variational ansatz for the flow equations comes from the l-bit picture [58, 59] and provides a method to solve the flow efficiently: only the first leading terms describing pairwise interactions among the localised integrals of motion in the MBL phase, are retained, while higher order effects are truncated and discarded. This represents an excellent description as long as the system is strongly localised. Given this ansatz for $H(l)$, the flow of the couplings is readily given by solution of $\frac{dH}{dl} = [\eta(l), H(l)]$. In other words, the flow brings the Hamiltonian of a single disordered fermionic wire (for instance, H_d in Eq. (1)) into an effectively diagonal one at the fixed point

$$\mathcal{H}(\infty) = \sum_i \tilde{h}_i n_i + \sum_{i,j} \tilde{\Delta}_{ij} n_i n_j, \quad (2)$$

with the dressed coupling at $l \rightarrow \infty$, given by $\tilde{h}_i = h_i(\infty)$ and $\tilde{\Delta}_{ij} = \Delta_{ij}(\infty)$. This, in turn, shows that the FE method effectively brings the Hamiltonian into the l-bit basis, with interaction couplings among the integrals of motion, spatially decaying in space as $\tilde{\Delta}_{ij} \propto \exp(-|i-j|/\xi)$. The values of \tilde{h}_i and $\tilde{\Delta}_{ij}$ depend on the specific disorder realization. Therefore, to consider disorder averaged quantities, the flow equations must be computed independently for each disorder realization.

As a measure of the quality of the truncation adopted, we follow Ref. [59], and we calculate the so-called second invariant, which is a quantity conserved by the exact unitary flow, and which therefore yields a measure of the fidelity of

the truncation associated to a given ansatz for the fixed point Hamiltonian of the flow (see the Supplemental Material (SM) for details).

This summarises the FE procedure for a single chain. In the two-chains model, described by the Hamiltonian (1), we extend the approach outlined above, and we build a family of unitary transformations parameterised by the running scale l , which effectively diagonalise (1) via a combined set of integrals of motion for the clean and disordered chains. The l -bit Hamiltonian resulting from such a transformation will therefore have the following form:

$$\begin{aligned} \mathcal{H}(\infty) = & \sum_i \tilde{h}_i^d n_i^d + \sum_{i,j} \tilde{\Delta}_{ij}^d n_i^c n_j^c + \\ & + \sum_i \tilde{h}_i^c n_i^c + \sum_{i,j} \tilde{\Delta}_{ij}^c n_i^c n_j^c + \\ & + \sum_{ij} \tilde{\Delta}_{ij}^I n_i^c n_j^d. \end{aligned} \quad (3)$$

As customary for flow equation methods [59], we Wick-order expectation values of operators with respect to a reference state ρ . The state ρ employed is a Boltzmann distribution with inverse temperature β , chemical potentials fixing particle densities $\langle n^d \rangle$ and $\langle n^c \rangle$, and Hamiltonian $H = \sum_i h_i^d n_i^d$. This state is chosen so we can easily control the energy density, β , and particle density distribution, $\langle n^d \rangle$.

By Wick-ordering the Hamiltonian at flow time $l = 0$, the clean and dirty chains pick up effective fields [64], given by

$$\begin{aligned} \bar{h}_i^d &= h_i^d + 2 \sum_j \Delta_{ij}^d \langle n_j^d \rangle + \sum_j \Delta_{ji}^I \langle n_j^c \rangle, \\ \bar{h}_i^c &= 2 \sum_j \Delta_{ij}^c \langle n_j^c \rangle + \sum_j \Delta_{ij}^I \langle n_j^d \rangle; \end{aligned} \quad (4)$$

their distribution depends on the dirty chain density, $\langle n^d \rangle$, the inter-chain coupling Δ^I , and the disorder, W , in the dirty chain. From the expressions of the fields in Eq. (4), it is natural to observe that, if the dirty chain is sufficiently disordered and the inter-chain couplings are sizeable, the clean chain will localize as result of the effective disordered field, \bar{h}_i^c .

To determine when the clean chain localizes, we solve for the l -bit Hamiltonian by numerically computing the flow of the couplings $\Delta^{c(d,l)}(l)$, $\bar{h}_i^{c(d)}(l)$ and $J_{ij}^{c(d)}(l)$ according to the first-order differential flow-equations presented in the SM. The flow is numerically evolved for a system with 24 clean and 24 dirty sites, and for a long enough flow-time that 1) the hoppings, $J_{ij}^{c(d)}(l)$, have become sufficiently small, and 2) there is no noticeable change in the flow of any other coupling. When both chains localize, our ansatz is sufficient to represent the diagonal Hamiltonian and the density-density couplings, $\Delta_{ij}^{c(d)}$, are exponentially suppressed in $|i - j|$, as it occurs in the applications of the Wegner flow to single disordered chains.

When either chain delocalizes, the l -bit Hamiltonian ansatz will be an insufficient representation of the effective Hamiltonian. Therefore we will use the growth of the second invariant as a sign that the system is exhibiting a tendency towards delocalization (as also done in Ref. [59]). We can then identify

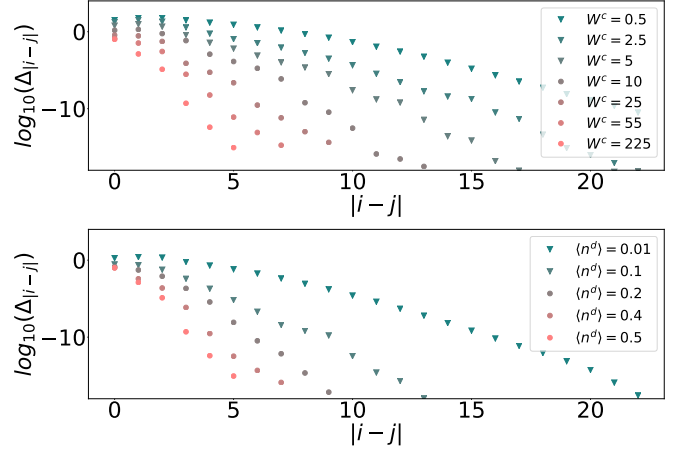


Figure 2: Instances of the MBL proximity effect: the plots show in logarithmic scale the spatial decay of pairwise couplings among the integrals of motion induced via proximity effect in the clean sector of the system. The parameters for which the change in the second invariant is larger and the method can no longer be trusted are plotted using triangles. The final density-density couplings $\Delta_{|i-j|}$ depicted here are averaged over the chain and 256 disorder realizations. In the top panel, we plot how the final density-density couplings depend on $W^c = \Delta^I/2J^c$ (J^c fixed) while in the bottom panel we plot their dependence on $\langle n^d \rangle$. In the top panel $\langle n^d \rangle = 0.5$ while in the bottom panel $W^c = 225$ ($\Delta^I = 45$ and $J^c = 0.1$). The remaining Hamiltonian parameters are $W = 60$, $J^d = \Delta^d = 0.1$, $\Delta^c = J^c = 0.1$, $\beta = 0.3$, and $\langle n^c \rangle = 0.1$. The above results are not affected by $\langle n^c \rangle$ since they are uniformly distributed in the reference state ρ and do not affect the disorder of the effective fields.

which chain delocalizes by comparing the suppression of the couplings $\tilde{\Delta}_{ij}^c$ and $\tilde{\Delta}_{ij}^d$ upon variation of system's parameters.

We are now in the position to discuss the different instances of the MBL proximity effect for the Hamiltonian (1). We focus on a model where the bare couplings involve only nearest-neighbour hopping and density-density interactions: $\Delta_{ij}^{c(d)} = \Delta^{c(d)} \delta_{i,j\pm 1}$, $J_{ij}^{c(d)} = J^{c(d)} \delta_{i,j\pm 1}$, and the inter-chain coupling is (as shown in Fig. 1) $\Delta_{ij}^I = \Delta^I \delta_{i,j}$.

In Fig. 2a, we show the decay in space of the asymptotic density-density couplings, $\tilde{\Delta}_{ij}$ in logarithmic scale. They demonstrate the exponential localization, and match the intuitive expectations for the onset of a MBL phase in the clean chain. As discussed in SM, the change in the second invariant for these parameters is small for the majority of disorder realizations and thus confirms the validity of the MBL proximity effect ansatz.

The top panel of Fig. 2 shows that by decreasing the inter-chain coupling, the final density-density couplings between the l -bits present a slower decay in space suggesting a departure from the MBL proximity phase. We use an effective disorder parameter, $W^c = \Delta^I/2J^c$, to compare with the (single) disordered Heisenberg chain which shows a transition at $W/J = 4$. By considering the second-invariant, we find [65] that the truncation produces minimal error for $W^c \gtrsim 10$ and the MBL proximity is well established. While for $W^c \lesssim 10$,

the error grows with decreasing W^c and suggests that somewhere in the range $W^c \lesssim 10$ the system undergoes a transition to a delocalized phase. In this limit, we have found that the final density-density couplings for the dirty-chain, $\tilde{\Delta}_{ij}^d$, are still strongly localized while those for the clean-chain are not. This suggests that the source of truncation error is due to the clean-chain becoming delocalized.

The bottom panel of Fig. 2b is one of the most interesting results of our analysis. Different curves correspond to different fermionic densities of the dirty component in (1). Numerical simulations are performed for a system with total fermionic density, $\langle n_{tot} \rangle \equiv \langle n^d \rangle + \langle n^c \rangle = 0.5$, and we vary $\langle n^d \rangle$ following a similar logic to the experiment in Ref. [61], where a complementary situation has been considered. There, the delocalising effect of the clean component on the dirty component has been experimentally observed in a mixture of collisionally coupled ultra-cold bosons in a two-dimensional optical lattice. Above a certain critical density of bosons, the clean component acts as an ergodic bath and destroys the features of the MBL phase in the dirty sector. Analogously, we find that a critical density of dirty fermions is required in order for the MBL systems to be sufficiently large to entail localisation in the clean component. The analysis of the second invariant identifies that the MBL proximity effect is well established for $\langle n^d \rangle > 0.25$, and suggests that for some value of $\langle n^d \rangle$ less than 0.25, the clean chain goes through a delocalization transition. It is important to note that we are unable to identify with accuracy the point of transition since our ansatz fails near it (see also Ref. [59]).

We also studied the effect of increasing the clean-chain hopping, J^c and the energy density, β of the reference state ρ . We found that our ansatz becomes inefficient and indicates the delocalization of the clean chain for large clean chain hopping, $J^c > 0.5$, and at large energy densities, $\beta < 0.05$. The dependence of localization on the hopping strength is similar to that in a standard MBL system, while the dependence on the energy density of the dirty chain is novel. This energy-density dependent behaviour is expected because the charge distribution in the dirty chain become more homogeneous at higher energy density.

These four for the breakdown of the MBL proximity effect ansatz can be understood in terms of the flow of J_{ij}^c and Δ_{ij}^c . As derived in the SM, J_{ij}^c is suppressed at a rate of $\propto \langle (\bar{h}_i^c - \bar{h}_j^c)^2 \rangle$, while the density-density couplings, Δ_{ij}^c delocalize at a rate $\propto J_{ij}^c$. The system localises or delocalizes depending on the competition between these two rates. If the hopping rates are too large ($J^c > 0.5$ for the parameters discussed above), the system delocalizes, while if the effective field is sufficiently strong and disordered, the tunnelling rates are suppressed. Eq. 4 shows that for the effective field to be sufficiently strong, the inter-chain coupling strength should also be sizeable. Furthermore, in order to be sensitive to strong disorder, the dirty chain state must have low energy densities and/or high density of particles [66]. The change in the effective field distribution is reflected in the localization

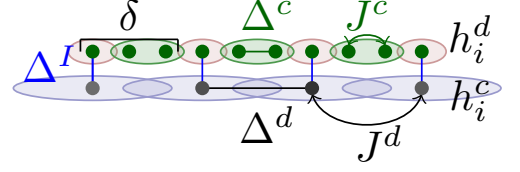


Figure 3: The portrait shows the dirty chain coupling to the clean one each $\delta = 3$ sites, and the integrals of motion emergent at intermediate time scales (n_k^d (blue), $n_{f,r=0}^c$ (red) and N_f (green)).

and delocalization of the clean chain as shown in Fig. 2.

We now discuss novel effects arising by tuning the coupling geometry illustrated in Fig. S5. In the geometry of Fig. S5 the clean system has δ times more degrees of freedom than the dirty chain, and each site in the dirty chain is coupled once every δ sites to the clean chain. This new geometry can still be studied using analogous flow equations to those employed above. The initial couplings, Δ_{ij}^I , can be easily written if we change the labelling of the clean chain sites. Noting that the clean chain is δ times longer than the dirty chain, we can label the dirty chain with $f = 0 \dots N_s - 1$, and conveniently reference the sites of the clean chain ($k = 0 \dots N_s\delta - 1$) with r , using $k = f\delta + r$. f labels the dirty sites and $r = 0 \dots \delta - 1$ is the number of sites away from the coupled site. We can now explicitly write the initial inter-chain coupling as $\Delta_{f,f'}^I = \Delta^I \delta_{f,f'} \delta_{r,0}$. This leads to an initial effective field $\bar{h}_{f,r}^c = \Delta^I \langle n_f^d \rangle \delta_{r,0}$. Therefore, hoppings $J_{f,r,f',r'}^c$ onto the coupled sites can be suppressed by $(\bar{h}_{f,r} - \bar{h}_{f',r'})^2$. Thus, by constructing a generator which only suppresses hopping on and off of the coupled site (see SM), we find a phase where tunnelling through the coupled sites is only possible by a next-nearest neighbour tunnelling of the form $J_{f,r=\delta-1,f'=f+1,r=1}^c$. We show [67] that the flow equations produce this coupling with size $(J^c(l=0))^2 / \bar{h}^c(l=0)$. Thus, on time scales shorter than $\bar{h}^c(l=0) / (J^c(l=0))^2$, the charge is unable to transport between neighbouring sets of uncoupled sites, and the total charge on these sets of uncoupled sites, $N_f = \sum_{r=1}^{\delta-1} n_{f,r}^c$, becomes an emergent local conserved charge. On time scales longer than $\bar{h}^c(l=0) / (J^c(l=0))^2$, the operator N_f is no longer conserved and the system may thermalize, depending on how large δ is and how disordered $\bar{h}_{f,r}^c$ is. For $\delta = 3$, the short time behaviour can be described by a non-interacting chain of spins-half ($N_f = 1$) or spins 0 ($N_f = 0$ or $N_f = 2$). In this case, the short time dynamics can be effectively described by a disordered transverse Ising model equipped with a set of emergent integrals of motion, as discussed in the SM.

A natural direction we are currently scrutinising consists in extending the FE method to capture physics akin to the one reported in the experiment of Ref. [61]. However, in order to have quantitative understanding of the delocalising impact of the clean environment on the disordered chain, one should assume that the clean chain is delocalized. We therefore plan to adapt the method changing our ansatz so that the clean chain

is diagonal in momentum space instead in real space, and preforming the flow equations on the dirty chain, so we can directly impact how the clean chain affects the l-bits [62]. Finally, it could be of interest to employ the FE method to study different setups of the onset for the MBL proximity effect. An appealing direction consists in studying a point-like, local coupling between a MBL segment of interacting, disordered fermions and a clean one. This would pave way to understanding the effect of the 'intrusion' of the localised system into the clean one, or viceversa, explore how a MBL system can act as an 'insulator' with respect to the clean segment. Analysis in this direction is ongoing [62].

Acknowledgements

S. P. K. and J. M. are indebted with S. J. Thomson and M. Schiro for helpful and clarifying discussions and exchanges on the flow equation method for MBL systems. We thank I. Bloch for inspiring discussions. JM is supported by the European Union's Horizon 2020 research and innovation programme under the Marie Skłodowska-Curie grant agreement No 745608 (QUAKE4PRELIMAT). This research was supported in part by the National Science Foundation under Grant No. NSF PHY-1748958.

This work is based upon work supported in part (RN, JM) by the Air Force office of Scientific Research under award number FA 9550-17-1-0183.

S. P. K. acknowledges financial support from the UC Office of the President through the UC Laboratory Fees Research Program, Award Number LGF-17- 476883

Los Alamos National Laboratory is managed by Triad National Security, LLC, for the National Nuclear Security Administration of the U.S. Department of Energy under Contract No. 89233218CNA000001

* Electronic address: jamirmarino@fas.harvard.edu

- [1] I. Bloch, J. Dalibard, and W. Zwerger, *Rev. Mod. Phys.* **80**, 885 (2008), URL <https://link.aps.org/doi/10.1103/RevModPhys.80.885>.
- [2] F. H. L. Essler and M. Fagotti, *J. Stat. Mech.* **2016**, 064002 (2016), URL <http://stacks.iop.org/1742-5468/2016/i=6/a=064002>.
- [3] P. Calabrese and J. Cardy, *J. Stat. Mech.* 064003 (2016).
- [4] C. J. Turner, A. A. Michailidis, D. A. Abanin, M. Serbyn, and Z. Papić, *Nature Physics*, **14**, 7, 745-749 (2016).
- [5] R. Nandkishore and D. A. Huse, *Annual Review of Condensed Matter Physics* **6**, 15 (2015), URL <http://dx.doi.org/10.1146/annurev-conmatphys-031214-014726>.
- [6] D. Abanin, E. Altman, I. Bloch, and M. Serbyn, *arXiv:1804.11065* (2018).
- [7] B. L. Altshuler, Y. Gefen, A. Kamenev, and L. S. Levitov, *Phys. Rev. Lett.* **78**, 2803 (1997), URL <https://link.aps.org/doi/10.1103/PhysRevLett.78.2803>.
- [8] D. Basko, I. Aleiner, and B. Altshuler, *Annals of Physics* **321**, 1126 (2006), ISSN 0003-4916, URL <http://www.sciencedirect.com/science/article/pii/S0003491605002630>.
- [9] I. V. Gornyi, A. D. Mirlin, and D. G. Polyakov, *Phys. Rev. B* **75**, 085421 (2007), URL <https://link.aps.org/doi/10.1103/PhysRevB.75.085421>.
- [10] A. Pal and D. A. Huse, *Phys. Rev. B* **82**, 174411 (2010), URL <http://link.aps.org/doi/10.1103/PhysRevB.82.174411>.
- [11] M. Znidaric, T. Prosen, and P. Prelovsek, *Phys. Rev. B* **77**, 064426 (2008), URL <http://link.aps.org/doi/10.1103/PhysRevB.77.064426>.
- [12] V. Oganesyan and D. A. Huse, *Phys. Rev. B* **75**, 155111 (2007), URL <http://link.aps.org/doi/10.1103/PhysRevB.75.155111>.
- [13] V. Khemani, R. Nandkishore, and S. L. Sondhi, *Nat Phys* **11**, 560 (2015), URL <http://dx.doi.org/10.1038/nphys3344>.
- [14] S. Gopalakrishnan, M. Müller, V. Khemani, M. Knap, E. Demler, and D. A. Huse, *Phys. Rev. B* **92**, 104202 (2015), URL <http://link.aps.org/doi/10.1103/PhysRevB.92.104202>.
- [15] J. H. Bardarson, F. Pollmann, and J. E. Moore, *Phys. Rev. Lett.* **109**, 017202 (2012), URL <https://link.aps.org/doi/10.1103/PhysRevLett.109.017202>.
- [16] S. D. Geraedts, R. Nandkishore, and N. Regnault, *Phys. Rev. B* **93**, 174202 (2016), URL <https://link.aps.org/doi/10.1103/PhysRevB.93.174202>.
- [17] V. Khemani, S. P. Lim, D. N. Sheng, and D. A. Huse, *Phys. Rev. X* **7**, 021013 (2017), URL <https://link.aps.org/doi/10.1103/PhysRevX.7.021013>.
- [18] Z.-C. Yang, A. Hama, S. M. Giampaolo, E. R. Mucciolo, and C. Chamon, *ArXiv e-prints* (2017), 1703.03420.
- [19] S. D. Geraedts, N. Regnault, and R. M. Nandkishore, *New Journal of Physics* **19**, 113021 (2017), URL <http://stacks.iop.org/1367-2630/19/i=11/a=113021>.
- [20] D. A. Huse, R. Nandkishore, V. Oganesyan, A. Pal, and S. L. Sondhi, *Phys. Rev. B* **88**, 014206 (2013), URL <http://link.aps.org/doi/10.1103/PhysRevB.88.014206>.
- [21] D. Pekker, G. Refael, E. Altman, E. Demler, and V. Oganesyan, *Phys. Rev. X* **4**, 011052 (2014), URL <http://link.aps.org/doi/10.1103/PhysRevX.4.011052>.
- [22] R. Vosk and E. Altman, *Phys. Rev. Lett.* **112**, 217204 (2014), URL <http://link.aps.org/doi/10.1103/PhysRevLett.112.217204>.
- [23] R. Vosk and E. Altman, *Phys. Rev. Lett.* **110**, 067204 (2013), URL <https://link.aps.org/doi/10.1103/PhysRevLett.110.067204>.
- [24] M. Serbyn, Z. Papić, and D. A. Abanin, *Phys. Rev. Lett.* **111**, 127201 (2013), URL link.aps.org/doi/10.1103/PhysRevLett.111.127201.
- [25] D. A. Huse, R. Nandkishore, and V. Oganesyan, *Phys. Rev. B* **90**, 174202 (2014), URL <http://link.aps.org/doi/10.1103/PhysRevB.90.174202>.
- [26] V. Ros, M. Müller, and A. Scardicchio, *Nuclear Physics B* **891**, 420 (2015), ISSN 0550-3213, URL <http://www.sciencedirect.com/science/article/pii/S0550321314003836>.
- [27] A. Chandran, A. Pal, C. R. Laumann, and A. Scardicchio, *ArXiv e-prints*: 1605.00655 (2016).
- [28] S. D. Geraedts, R. N. Bhatt, and R. Nandkishore, *Phys. Rev. B* **95**, 064204 (2017), URL <http://link.aps.org/doi/10.1103/PhysRevB.95.064204>.
- [29] S. A. Parameswaran and S. Gopalakrishnan, *ArXiv e-prints*

- (2016), 1608.00981.
- [30] J. Z. Imbrie, Phys. Rev. Lett. **117**, 027201 (2016), URL <https://link.aps.org/doi/10.1103/PhysRevLett.117.027201>.
 - [31] M. Schreiber, S. S. Hodgman, P. Bordia, H. P. Lüschen, M. H. Fischer, R. Vosk, E. Altman, U. Schneider, and I. Bloch, Science **349**, 842 (2015).
 - [32] P. Bordia, H. P. Lüschen, S. S. Hodgman, M. Schreiber, I. Bloch, and U. Schneider, Phys. Rev. Lett. **116**, 140401 (2016), URL <https://link.aps.org/doi/10.1103/PhysRevLett.116.140401>.
 - [33] J. Choi, S. Hild, J. Zeiher, P. Schauss, A. Rubio-Abadal, T. Yefsah, V. Khemani, D. A. Huse, I. Bloch, and C. Gross, Science **352**, 1547 (2016).
 - [34] M. Rispoli, A. Lukin, R. Schittko, S. Kim, M. E. Tai, J. Leonard, and M. Greiner, arXiv:1812.06959 (2018).
 - [35] P. Roushan, C. Neill, J. Tangpanitanon, V. M. Bastidas, A. Megrant, R. Barends, Y. Chen, Z. Chen, B. Chiaro, A. Dunsworth, et al., Science **358**, 1175-1179 (2017).
 - [36] R. Nandkishore, S. Gopalakrishnan, and D. A. Huse, Phys. Rev. B **90**, 064203 (2014), URL <https://link.aps.org/doi/10.1103/PhysRevB.90.064203>.
 - [37] R. Nandkishore and S. Gopalakrishnan, Annalen der Physik pp. 1521-3889 (2016), URL <http://dx.doi.org/10.1002/andp.201600181>.
 - [38] S. Gopalakrishnan and R. Nandkishore, Phys. Rev. B **90**, 224203 (2014), URL <https://link.aps.org/doi/10.1103/PhysRevB.90.224203>.
 - [39] S. Banerjee and E. Altman, Phys. Rev. Lett. **116**, 116601 (2016), URL <https://link.aps.org/doi/10.1103/PhysRevLett.116.116601>.
 - [40] M. H. Fischer, M. Maksymenko, and E. Altman, Phys. Rev. Lett. **116**, 160401 (2016), URL <https://link.aps.org/doi/10.1103/PhysRevLett.116.160401>.
 - [41] E. Levi, M. Heyl, I. Lesanovsky, and J. P. Garrahan, Phys. Rev. Lett. **116**, 237203 (2016), URL <https://link.aps.org/doi/10.1103/PhysRevLett.116.237203>.
 - [42] M. Medvedyeva, T. Prosen, and M. Znidaric, Phys. Rev. B **93**, 094205 (2016), URL <https://link.aps.org/doi/10.1103/PhysRevB.93.094205>.
 - [43] W. De Roeck and F. Huveneers, arXiv 1608.01815 (2016).
 - [44] D. J. Luitz, F. Huveneers, and W. De Roeck, Phys. Rev. Lett. **119**, 150602 (2017), URL <https://link.aps.org/doi/10.1103/PhysRevLett.119.150602>.
 - [45] P. Ponte, C. Laumann, D. Huse, and A. Chandran, Philosophical Transactions A (2017).
 - [46] S. Lorenzo, T. Apollaro, G. M. Palma, R. Nandkishore, A. Silva, and J. Marino, Phys. Rev. B **98**, 054302 (2018), URL <https://link.aps.org/doi/10.1103/PhysRevB.98.054302>.
 - [47] H. P. Lüschen, P. Bordia, S. S. Hodgman, M. Schreiber, S. Sarkar, A. J. Daley, M. H. Fischer, E. Altman, I. Bloch, and U. Schneider, Phys. Rev. X **7**, 011034 (2017), URL <https://link.aps.org/doi/10.1103/PhysRevX.7.011034>.
 - [48] R. Nandkishore, Phys. Rev. B **92**, 245141 (2015), URL <https://link.aps.org/doi/10.1103/PhysRevB.92.245141>.
 - [49] K. Hyatt, J. R. Garrison, A. C. Potter, and B. Bauer, Physical Review B **95** (2016).
 - [50] J. Marino and R. M. Nandkishore, Phys. Rev. B **97**, 054201 (2018), URL <https://link.aps.org/doi/10.1103/PhysRevB.97.054201>.
 - [51] R. Vosk, D. A. Huse, and E. Altman, Phys. Rev. X **5**, 031032 (2015), URL <https://link.aps.org/doi/10.1103/PhysRevX.5.031032>.
 - [52] A. C. Potter, R. Vasseur, and S. A. Parameswaran, Phys. Rev. X **5**, 031033 (2015), URL <https://link.aps.org/doi/10.1103/PhysRevX.5.031033>.
 - [53] P. T. Dumitrescu, R. Vasseur, and A. C. Potter, Phys. Rev. Lett. **119**, 110604 (2017), URL <https://link.aps.org/doi/10.1103/PhysRevLett.119.110604>.
 - [54] T. Thiery, F. Huveneers, M. Müller, and W. De Roeck, Phys. Rev. Lett. **121**, 140601 (2018), URL <https://link.aps.org/doi/10.1103/PhysRevLett.121.140601>.
 - [55] S.-X. Zhang and H. Yao, Phys. Rev. Lett. **121**, 206601 (2018), URL <https://link.aps.org/doi/10.1103/PhysRevLett.121.206601>.
 - [56] A. Goremykina, R. Vasseur, and M. Serbyn, Phys. Rev. Lett. **122**, 040601 (2019), URL <https://link.aps.org/doi/10.1103/PhysRevLett.122.040601>.
 - [57] S. Kehrein, The flow equation approach to many-particle systems (Springer, 2007).
 - [58] D. Pekker, B. K. Clark, V. Oganesyan, and G. Refael, Phys. Rev. Lett. **119**, 075701 (2017).
 - [59] S. Thomson and M. Schiro, arXiv:cond-mat pp. Phys. Rev. B **97**, 060201 (2018).
 - [60] F. Wegner, Annalen der Physik **506**, 77 (1994).
 - [61] A. Rubio-Abadal, J. Choi, J. Zeiher, S. Hollerith, J. Rui, I. Bloch, and C. Gross, arXiv:1805.00056 (2018).
 - [62] S. Kelly and et al., in preparation (2019).
 - [63] C. Monthus, Journal of Physics A: Mathematical and Theoretical **49**, 305002 (2016).
 - [64] See Supplemental Material at [URL will be inserted by publisher] for the derivation of the effective field
 - [65] See Supplemental Material at [URL will be inserted by publisher] for a discussion of the second invariant.
 - [66] See Supplemental Material at [URL will be inserted by publisher] for a computation of the statistics for the effective field.
 - [67] See Supplemental Material at [URL will be inserted by publisher] for a derivation of the second order tunnelling magnitude.

Supplemental Materials: Exploring many-body localisation in open quantum systems via Wegner-Wilson flows

The supplemental material is organized as follows. In Section , we discuss the approximations used in the ansatz for the flowing hamiltonian. In Section , we sketch the derivation of the flow equations and discuss the effect of the approximation Scheme. In Section , we discuss the second invariant, a quantity used to test our approximation scheme . In Section , we compute the statistics of the effective field distribution of the clean chain and show how it depends on the energy and number density. In Section , we discuss the phases that can emerge due to a separation of time scales that arises due to the non-trivial inter-chain coupling geometry discussed in the paper. Finally, in Section we discuss some of the details of the numerical implementation of the flow equations.

THE PROXIMITY EFFECT ANSATZ.

As discussed in the introduction, the flow equations describe a sequence of infinitesimal unitary transforms which transform a hamiltonian with off diagonal components $V(l)$ to one which is diagonal. The main technical difficulty is identifying the ansatz which captures most of the correlations but still yields feasible computations. The ansatz we choose is:

$$\begin{aligned}
 H_0 &= H^c + H^d + H^I \\
 H^c &= \sum_{ij} \Delta_{ij}^c(l) : n_i^c n_j^c : + \sum_k \tilde{h}_k^c(l) : n_k^c : \\
 H^d &= \sum_{ij} \Delta_{ij}^d(l) : n_i^d n_j^d : + \sum_k \tilde{h}_k^d(l) : n_k^d : \\
 H^I &= \sum_{ij} \Delta_{ij}^I(l) : n_i^c n_j^d : \\
 V &= \sum_{ij} J_{ij}^c(l) : c_i^\dagger c_j : + \sum_{ij} J_{ij}^d(l) : d_i^\dagger d_j :
 \end{aligned} \tag{S1}$$

where $: A :$ denotes the wick-ordering [57] of an operator A with respect to a Gaussian state ρ , and for clarity the first index in Δ_{ij} will always index the clean chain.

This ansatz has a symmetry: $c \leftrightarrow d$, $\Delta_{ij}^I \leftrightarrow \Delta_{ji}^I$. Via this substitution, an equation valid for the clean chain can be turned into one valid for the dirty chain as long as chain dependent simplifications aren't performed. For the rest of the supplemental material, all the results will be in terms of the clean chain, and the above symmetry will allow one to get the corresponding equations for the dirty chain. If the super script is not given it is assumed to be c .

This ansatz relies on two approximation methods. The first is Wick-ordering and allows to focus on a specific set of basis states, relying on the assumption that other states are not significantly mixed with this set during the sequence of unitary transformation. The second is a perturbative expansion which relies on $J^{c(d)}$ and $\Delta^{c(d)}$ being small. We will discuss both in the following two subsections.

Wick-ordering

The primary approximation in the ansatz Eq S1 is in dropping all $n > 2$ particle operators. This is justified by using a basis of Wick-ordered operators to define the ansatz. For clarity, we point out there are two vector spaces in consideration: 1) the Hilbert space of physical states and 2) the operator algebra acting on the Hilbert space of physical states. The Wick-ordered operators form a basis for the operator algebra and are defined in terms of the contractions:

$$C_{kl} = \text{tr}[A_k A_l \rho], \tag{S2}$$

and the recursion relation:

$$: A_k O := A_k : O : - \sum_l C_{kl} : \frac{\partial O}{\partial A_l} \tag{S3}$$

where $: O :$ denotes a Wick-ordered operator expressed as a polynomial of creation and annihilation operators, $A_{k(l)}$. The couplings $\Delta_{ij}^{c(d,I)}$, $\tilde{h}_k^{c(d)}$ and $J_{ij}^{c(d)}$ form a well defined representation of the hamiltonian.

Wick-ordering is performed so the truncation errors made in this approximation are minimized [57] for the Hilbert-space spanned by all 2-particle excitations away from the state ρ . For Wick-ordering to reduce truncation errors, the state ρ must have Gaussian form. So we choose it to be a Boltzmann distribution with respect to the Gaussian part of $H_0(l=0)$:

$$\rho = \frac{1}{Z} e^{-\beta(-\mu^c \sum_i n_i^c + \sum_i (h_i^d - \mu^d) n_i^d)} \quad (\text{S4})$$

where μ^c and μ^d are chosen to fix the total average density of the clean and dirty chain.

When performing Wick-ordering with respect to this state, the hamiltonian in Eq (S1), has a different coupling \bar{h}_k^c then the bare field h_k^c because of the relation between the Wick-ordered density-density operator and the bare density-density operator:

$$\begin{aligned} : n_i n_j : &= n_i n_j - C_{ii} n_j - C_{jj} n_i - C_{ii} C_{jj} \\ &= n_i n_j - \langle n_i \rangle n_j - \langle n_j \rangle n_i - \langle n_i \rangle \langle n_j \rangle. \end{aligned} \quad (\text{S5})$$

The coupling \bar{h}_k^c is related to the bare field h_k^c by:

$$\bar{h}_i^c = h_i^c + 2 \sum_j \Delta_{ij}^c \langle n_j^c \rangle + \sum_j \Delta_{ij}^I \langle n_j^d \rangle. \quad (\text{S6})$$

A corresponding equation is valid for the dirty chain given by $c \leftrightarrow d$, $\Delta_{ij}^I \leftrightarrow \Delta_{ij}^c$.

In the flow equations, we will track the coupling to the Wick-ordered operator, $\bar{h}_i^c(l)$, which have an initial value of $h_i^c(l=0) + 2 \sum_j \Delta_{ij}^c(l=0) \langle n_j^c \rangle + \sum_j \Delta_{ij}^I(l=0) \langle n_j^d \rangle$. Thus the disorder in the reference state density $\langle n_i^d \rangle$ will determine how the flow of the clean chain localizes.

Pertubative expansion

In addition to dropping 4-particle and higher-order operators from the ansatz, we have dropped off-diagonal terms such as: $n_k^c c_i^\dagger c_j$ and $c_k^\dagger c_l c_i^\dagger c_j$. Including these terms requires keep track of an $O(N_s^3)$ and $O(N_s^4)$ number of couplings, so we work in the limit where J^c and Δ^c are small so dropping these terms is justified. To see this, we first write define our expansion parameters λ_J and λ_Δ :

$$\begin{aligned} H &= H^c + H^d + \hat{\Delta}^I \\ H^c &= \lambda_J \hat{J}^c + \lambda_\Delta \hat{\Delta}^c + \hat{h}^c \\ H^d &= \lambda_J \hat{J}^d + \lambda_\Delta \hat{\Delta}^d + \hat{h}^d, \end{aligned} \quad (\text{S7})$$

where $\hat{\Delta}^I$, \hat{J}^c , $\hat{\Delta}^c$ and \hat{h}^c are the operators associated with the sums in Eq. S1: $\hat{h}^c = \sum_k \bar{h}_k^c : n_k^c :$. We can then identify three contributions to the generator $\eta = [V, H_0]$ and their perturbative order:

$$\begin{aligned} \eta_{h^c} &= \lambda_J [\hat{J}^c, \hat{h}^c] \\ \eta_\Delta &= \lambda_J \lambda_\Delta [\hat{J}^c, \hat{\Delta}^c] \\ \eta_{I^c} &= \lambda_J [\hat{J}^c, \hat{\Delta}^I]. \end{aligned} \quad (\text{S8})$$

The perturbative order of the contributions to the flow equation, $[H, \eta]$, are then shown in table I. In the next section we describe the derivation of these commutators and list the resulting types of operators in table II. The ansatz we chose, drops contributions to the flow equations of second order in a small coupling. It is important to note, that if a hopping operator is produced by $[H, \eta]$ that is second order in λ_J , then its contribution to the flow of $J_{ij}(l)$ is first order because $J_{ij}(l)$ is already small of order λ_J . Similar arguments hold for the contribution to $\Delta_{ij}(l)$. Comparing table I with table II, we see that only the commutators $[\eta_f, \hat{\Delta}^I]$ and $[\eta_I, \hat{\Delta}^I]$ produce a term dropped by the ansatz which is first order in the expansion parameters. This term is the inter-chain correlated hopping operator, $n_k^c c_i^\dagger c_j$.

Dropping these operators requires further justification based on the fact that the bare hamiltonian does not contain these terms. Since the couplings for these operators are initially zero, it will remain small (less than $O(\lambda_J)$) at the beginning of the flow and only contribute to the diagonal hamiltonian at an order less than $O((\lambda_J)^2)$. Dropping this operator is justified as long as its coupling does not grow to a significant size later in the flow. By checking the second invariant, we find this to be the case when the system is strongly localized.

	h	J	Δ	Δ^I
η_h	λ_J	λ_J^2	$\lambda_J \lambda_\Delta$	λ_J
η_Δ	$\lambda_J \lambda_\Delta$	$\lambda_J^2 \lambda_\Delta$	$\lambda_J \lambda_\Delta^2$	$\lambda_J \lambda_\Delta$
η_I	λ_J	λ_J^2	$\lambda_J \lambda_\Delta$	λ_J

Table I: Perturbative order of contribution: the entries in this table correspond to the perturbative order of the commutators described in Table II.

THE FLOW EQUATIONS.

The commutators for the generator can be computed using the rules for wick-ordered commutators [57]. Grouping them on the basis of the resulting operator, we get:

$$\begin{aligned}
\eta_{fc} &= \sum_{ij} F_{ij} : c_i^\dagger c_j : \\
\eta_{\Delta^c} &= \sum_{ijk} \Gamma_{ijk}^c : c_k^\dagger c_k c_i^\dagger c_j : \\
\eta_I^c &= \sum_{ijk} \Gamma_{ijk}^I : d_k^\dagger d_k c_i^\dagger c_j :
\end{aligned} \tag{S9}$$

with

$$\begin{aligned}
F_{ij}^c &= F_{ij}^{\Delta^c} + F_{ij}^{h^c} \\
F_{ij}^{h^c} &= J_{ij}^c (\bar{h}_i^c - \bar{h}_j^c) \\
F_{ij}^{\Delta^c} &= 2J_{ij}^c \Delta_{ij} (n_i - n_j)
\end{aligned} \tag{S10}$$

and

$$\begin{aligned}
\Gamma_{ijk}^c &= 2J_{ij}^c (\Delta_{ik}^c - \Delta_{jk}^c) \\
\Gamma_{ijk}^I &= J_{ij}^c (\Delta_{ik}^I - \Delta_{jk}^I).
\end{aligned} \tag{S11}$$

These 3(6) generators are commuted with the 4(7) terms in the hamiltonian for a total of 12(24 for both clean and dirty chains) different contributions to the flow equations. To which couplings in the ansatz these commutators contribute, are summarized in table II. The initials C.H., C.H.I., 3T and F.S. stand for correlated hopping ($: n_k^c c_i^\dagger c_j :$), inter-chain correlated hopping ($n_k^d c_i^\dagger c_j$), a three-particle operator, and full scattering ($c_k^\dagger c_l^\dagger c_i c_j$). Each one of these terms are dropped by the ansatz and are justified in Section . The remaining terms contain contributions to the flow of the couplings, $J_{ij}^{c(d)}(l)$, $\Delta_{ij}^{c(d,I)}(l)$ and $\bar{h}_k^{c(d)}(l)$. The contributions from the first two column are discussed in Section , while the subtleties in including contributions from the third and forth column are discussed in Section .

Perturbatively safe contributions to the Flow equations

The contribution $[\eta_h, \hat{h}]$ is order λ_J and only produces terms that are part of the ansatz. Its simplicity will provide a useful example for the methods used in treating the correlated-hopping operator. This contribution is given by:

$$\begin{aligned}
\sum_{ijn} h_n^c F_{ij}^c [: c_i^\dagger c_j : , : c_n^\dagger c_n :] = \\
- \sum_{ij} F_{ij}^c (\bar{h}_i^c - \bar{h}_j^c) : c_i^\dagger c_j :
\end{aligned} \tag{S12}$$

Substituting F_{ij} from Eq. S11, we get a contribution to the flow of the hopping J_{ij} as:

$$\frac{dJ_{ij}}{dl} = -J_{ij}(\bar{h}_i - \bar{h}_j)^2 - J_{ij}2\Delta_{ij}(n_i - n_j)(\bar{h}_i - \bar{h}_j).$$

	h	J	Δ	Δ^I
η_f (1)	J_{ij}	J_{ij}, h_i	C.H.	C.H.I
η_f (2)	C	C	J_{ij}	
η_Δ (1)	C.H.	$\Delta_{i,j}$, C.H., F.S.	3T	3.T.
η_Δ (2)		J_{ij}, h_i	C.H.	C.H.I
η_Δ (3)			J_{ij}	0
η_I (1)	C.H.I	$\Delta_{i,j}^I$, C.H.I., F.S.I	3T	3T
η_I (2)		$J_{ij}^{d(c)}, h_i^{d(c)}$	C.H.	C.H.I
η_I (3)			0	$J_{ij}^{c(d)}$

Table II: This table lists the set of generators, η_i , from one chain in the first column and the terms in the hamiltonian H_i which act on the same chain in the first row. The entries of the table list which couplings in the ansatz hamiltonian the commutator $[\eta_i, H_i]$ contribute to. The number in parenthesis in the first column indicate the number of contractions performed in that contribution to the commutator (see the rules in [57] for more detail). The blue highlighted terms are present regardless of the form of the contractions. The contributions highlighted in green are those that appear due to an inhomogeneous distribution of n_i .

This equation is valid for both the clean and dirty chain. The first term is how the hoppings J_{ij} are suppressed by the disorder onsite fields. The second term shows how the density-density interaction also effects localization through the contractions. The contribution from the inter-chain interaction is hidden in the effective field \bar{h}_i .

The contribution to the flow equation from the commutator $[V, \eta]$ are all order λ_J^2 , and thus dropping terms in the ansatz from these contributions is justified. These contributions which are not dropped are significantly more complicated then the one in Eq. S12, but can be carefully computed using the rules in [57]. Doing so results in the flow equations:

$$\begin{aligned}
\frac{dh_k^c}{dl} &= \sum_i 2J_{ik}^2 [(h_k - h_i) + 2\Delta_{ik}(n_k - n_i)] + 2 \sum_{ij} (J_{ij})^2 (\Delta_{kj} - \Delta_{ki})(n_j - n_i) \\
&\quad + \sum_{ij} (J_{ij}^d)^2 (\Delta_{kj}^I - \Delta_{ki}^I)(n_j^d - n_i^d) \\
\frac{dJ_{ij}^c}{dl} &= -J_{ij}(h_i - h_j)^2 - 2J_{ij}\Delta_{ij}(n_i - n_j)(h_i - h_j) - \sum_k J_{ik}J_{kj}(2h_k - h_i - h_j) \\
&\quad - 2 \sum_k J_{ik}J_{kj}[\Delta_{ij}(n_i + n_j - 2n_k) + 2\Delta_{ki}(n_k - n_i) + 2\Delta_{kj}(n_k - n_j)] \\
\frac{d\Delta_{ij}^c}{dl} &= 2 \sum_{k \neq i, j, l=i, j} J_{lk}^2 (\Delta_{ij} - \Delta_{kl'}) \\
\frac{d\Delta_{ij}^I}{dl} &= 2 \sum_k (J_{jk}^d)^2 (\Delta_{ij}^I - \Delta_{ik}^I) + 2 \sum_k (J_{ik}^c)^2 (\Delta_{ij}^I - \Delta_{kj}^I)
\end{aligned} \tag{S13}$$

where the couplings without a chain label are assumed to be clean, and the flow for the dirty couplings can be found by swapping the clean and dirty couplings ($c \leftrightarrow d$, $\Delta_{ij}^I \leftrightarrow \Delta_{ij}^c$). In comparison to Ref. [59], this does not include the 3 contraction contribution as this comes from the commutator $[\eta, \Delta^c]$ which will be computed in the next section. The only other difference is an extra set of 2 contraction terms which would be zero at the infinite temperature limit they assumed.

Correlated Hopping Operators

In this section we consider the flow contribution from the third and fourth column of table II. The derivation of these terms can be simplified by the following relations for wick-ordered operators:

$$\begin{aligned}
:n_k^c d_i^\dagger d_j : &= :n_k^c :: d_i^\dagger d_j : \\
:n_k^c c_i^\dagger c_j : &= A_{ijk}(n^c, :n^c:) :c_i^\dagger c_j :,
\end{aligned} \tag{S14}$$

where A is defined as:

$$A_{ijk}(n^c, :n^c:) = :n_k^c : - \delta_{ki} + \langle n_k^c \rangle (\delta_{ki} + \delta_{kj}). \tag{S15}$$

We can now express the generators and diagonal hamiltonian in a form similar to h^c and η_h in terms of a set of effective field operators:

$$\begin{aligned} : h_i^{ec} : &:= \sum_k \Delta_{ik}^I : n_k^d : \\ : h_i^{ac} : &:= \sum_k \Delta_{ik}^c : n_k^c : \\ : h_{s=i/j, ij}^{oc} : &:= \sum_k \Delta_{sk}^c : A_{ijk}^d : . \end{aligned} \quad (\text{S16})$$

With these fields, we can rewrite the generators η_Δ and η_{Δ^I} in a form similar to η_h :

$$\begin{aligned} \eta_{\Delta^c} &= \sum_{ij} : \Gamma_{ij}^c : : c_i^\dagger c_j : \\ \eta_{I^c} &= \sum_{ij} : \Gamma_{ij}^{I^c} : : c_i^\dagger c_j : , \end{aligned} \quad (\text{S17})$$

with

$$\begin{aligned} : \Gamma_{ij}^c : &= 2J_{ij}^c (: h_{i,ij}^{oc} : - : h_{j,ij}^{oc} :) \\ : \Gamma_{ij}^{I^c} : &= J_{ij}^c (: h_i^{ec} : - : h_j^{ec} :) . \end{aligned} \quad (\text{S18})$$

The total generator can now be written as

$$\begin{aligned} \eta^c &= \sum_{ij} : F_{ij}^{T^c} : : c_i^\dagger c_j : \\ : F_{ij}^{T^c} : &= : F_{ij}^c : + : \Gamma_{ij}^c : + : \Gamma_{ij}^I : . \end{aligned} \quad (\text{S19})$$

We can also rewrite the interaction operators as:

$$\begin{aligned} \Delta^I &= \sum_{ij} \Delta_{ij}^I : n_i^c : : n_j^d : = \sum_k : h^{ec} : : n_k^c : \\ &= \sum_k : h^{ed} : : n_k^d : \\ \Delta^c &= \sum_k : h_k^{ac} : : n_k^c : . \end{aligned} \quad (\text{S20})$$

The diagonal part of the clean chain is now written:

$$\begin{aligned} H_0^c &= \sum_k : h_k^T : : n_k^c : \\ : h_k^T : &= : h_k^c : + : h_k^{ec} : + : h_k^{ac} : . \end{aligned} \quad (\text{S21})$$

The terms in the flow equations, $[\eta, H_0]$, can now be written in a form similar to Eq. [S12](#):

$$\begin{aligned} [\eta^c, H_0^c] &= \\ &= \sum_{ij} : F_{ij}^{T^c} : (: h_j^{T'} : - : h_i^{T'} :) : c_i^\dagger c_j : \\ : h_k^{T'} : &= : h_k^c : + : h_k^{ec} : + 2 : h_k^{ac} : , \end{aligned} \quad (\text{S22})$$

where the factor of 2 comes from

$$\begin{aligned} &[\sum_k : h_k^{ac} : , : n_k : , O] \\ &= \sum_k [: h_k^{ac} : , O] : n_k : + \sum_k : h_k^{ac} : [: n_k : , O] \\ &= 2 \sum_k : h_k^{ac} : [: n_k : , O] . \end{aligned} \quad (\text{S23})$$

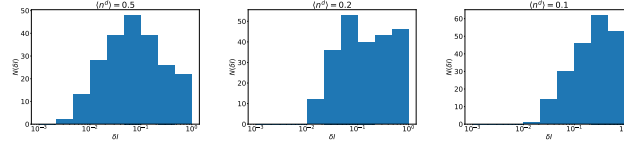


Figure S1: Histograms of the change in the second invariant as $\langle n^d \rangle$ is swept through transition. The remaining Hamiltonian parameters are $W = 60$, $J^d = \Delta^d = 0.1$, $\Delta^c = J^c = 0.1$, $\beta = 0.3$, and $\langle n^c \rangle = 0.1$.

The contribution from the constant part of F_{ij}^{Tc} and the constant part of $h_{i(j)}^{T'}$ are the contribution in blue of Eq. S14. Contracting the remaining terms produces a product of 6, 4 and 2 wick-ordered fermion operators expected in the third and fourth column of Table II

These operators are all off diagonal with respect to $H_0(l)$. With in the 4-particle truncation, we should keep the 4 and 2 Wick-ordered fermion operators. These operators are of the form of a hopping, $c_i^\dagger c_j$ and a correlated hopping, $n_k c_i^\dagger c_j$. This generator is constructed to suppress the hoppings which change energy due to the density-density interaction. It has the side effect of producing a correlated hopping interaction at the same rate the hopping, J_{ij} , is suppressed. Thus if we drop the delocalizing effects of the correlated hopping operators, we arbitrarily bias the localizing effects captured by the contribution to the hopping term. To avoid this we include neither contribution. This is consistent with our private communication with the authors of [59].

In the limit when the effective field is dominant in localising the system, the effects from these terms are negligible. It is at the transition point, that dropping both these terms is a poor approximation. This is verified by our numerical considerations on the second invariant.

SECOND INVARIANT

The approximation performed above does not have a neat control parameter: it relies on the assumption that the correlated hopping term never grows to a size comparable to $O(\lambda_J)$. To test its validity, we use the invariance of the quantity $\text{Tr} [H(l)^2]$. For a spin-half chain or spinless fermion chain, the small local Hilbert space allows for a simple expression for this quantity [59, 63]:

$$\text{Tr} [H(l)^2] = \sum_{ij,r=c,d} (J_{ij}^r)^2 + (\Delta_{ij}^r)^2 + \Delta_{ij}^I + \sum_{k,r=c,d} (\bar{h}_k^r)^2. \quad (\text{S24})$$

We quantify its change by using:

$$\delta I = 2 \frac{\text{Tr} [H(l = \infty)^2] - \text{Tr} [H(l = 0)^2]}{\text{Tr} [H(l = \infty)^2] + \text{Tr} [H(l = 0)^2]}. \quad (\text{S25})$$

We refer to this quantity as the change in the second invariant, and note that it measures the extent to which the approximation breaks the unitarity of the transformation.

As the transformation performed by the flow equations depends on the disorder realization, δI varies from sample-to-sample. The left panel of Fig. S1 shows the distribution of δI for a system in which the ansatz preserves the unitary transform for the majority of disorder realizations, while the right panel shows the distribution for a system for which the ansatz fails for the majority of disorder realizations. To distinguish between the two we compute the median of δI for a particular disorder realization, since the mean is artificially weighted by these few trials with large second invariant. As shown in Fig. S2, the median δI shows that the MBL proximity effect ansatz becomes worse for decreasing Δ^I and $\langle n^D \rangle$. Here we see that for $W^c > 10$ and for $\langle n^d \rangle > 0.25$, the median second invariant is small and relatively unaffected by changes in W^c and $\langle n^d \rangle$, demonstrating the validity of the many body proximity effect Ansatz. While for small $W^c < 10$ and small $\langle n^d \rangle < 0.25$, the error made by truncation is large suggestive of a transition to delocalization somewhere below these values.

The large sample-to-sample variation of the second invariant suggests the presence of regions not captured by the MBL proximity effect ansatz. Future work could potentially attempt to reduce the second invariant for these disorder realizations by including the correlated-hopping couplings in the ansatz or keeping track of resonances in the Wick ordered reference state.

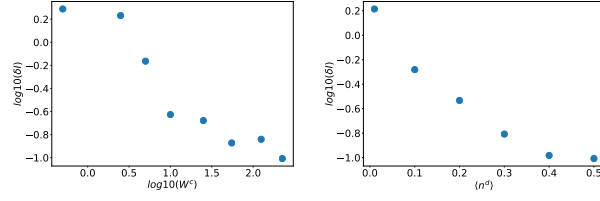


Figure S2: Median change in the second invariant as $\langle n^d \rangle$ and W^c are swept through the transition. W^c is plotted on a log scale since we vary it over 2 orders of magnitude. The remaining Hamiltonian parameters are $J^d = \Delta^d = 0.1$, $\Delta^c = J^c = 0.1$, $\beta = 0.3$, and $\langle n^c \rangle = 0.1$. In the left Plot $\langle n^d \rangle = 0.5$ and on the right plot, $W = 60$

EFFECTIVE FIELDS AS A FUNCTION OF TEMPERATURE AND NUMBER DENSITY

By considering Fig. S3, we can see how the selected energy density β^{-1} and total density on the dirty chain $\langle n^d \rangle$, influence the effective field distribution for a fixed Δ^I . At higher energy densities and lower dirty-chain particle densities, the effective field distribution has a single peak, demonstrating lack of disorder, while the uncertainty in the effective field strength is largest at lower energy density and higher dirty-chain particle density. We compute these distributions by randomly sampling the dirty chain disorder field and using the Boltzmann distribution, Eq. S4, to compute the dirty chain densities and clean chain effective fields.

EFFECTS OF INTER-CHAIN COUPLING GEOMETRY: NON-ERGODIC PHASES ALTERNATIVE TO MBL

In the text we discussed the emergence of a separation of time scales due to the non-trivial inter-chain coupling geometry shown Fig. S5. This coupling geometry is described by labelling the dirty chain with $f = 0 \dots N_s - 1$, and conveniently reference the sites of the clean chain ($k = 0 \dots N_s \delta - 1$) with r , using $k = f\delta + r$. The initial inter-chain coupling is then written as $\Delta_{f,r,f'} = \Delta^I \delta_{f,f'} \delta_{r,0}$.

On intermediate time scales, the system behaved as if there were a set of emergent integrals of motion on the uncoupled sites in the clean chain. While at long times, the clean chain thermalizes. In this section we first calculate the time scale at which the integrals of motion breakdown, and the possible phases that could exist at earlier times.

Estimation of Long Range Tunnelling and Separation of Time Scales

In the main text, we argued how an initial effective field, $\bar{h}_{f,r}^c = \Delta^I \langle n_f^d \rangle \delta_{r,0}$, suppresses hoppings, $J_{f,r,f',r'}^c$, onto the coupled sites at a rate of $(\bar{h}_{f,r} - \bar{h}_{f',r'})^2$. We can see this by observing in Fig. S4 how $J_{k,k'}^c(l)$ evolves as a function of the flow parameter l . The right panel of Fig. S4 shows the suppression of the hopping between a coupled sites $f, r = 0$ and an uncoupled site $f, r = 1$, while the left panel of Fig. S4 shows the hopping between two uncoupled sites, $f, r = 1$ and $f' = f, r = 2$, remaining constant. This unsuppressed hopping is due to $(\bar{h}_{f,r=1} - \bar{h}_{f'=f,r'=2})^2 = 0$.

Using the same flow equations for simpler geometry, the density-density couplings on the uncoupled sites will diverge due to the unsuppressed hoppings on the uncoupled sites. This is also observed in the left panel of Fig. S4. This breakdown of the flow

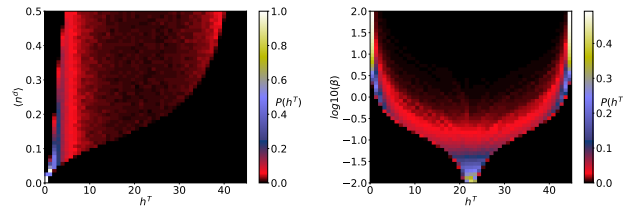


Figure S3: Distribution of the clean-chain effective field as $\langle n^d \rangle$ and β are varied at a fixed inter-chain coupling, $\Delta^I = 45$. At $\beta = 0.3$ the distribution of the effective field strength is most similar to a box-distribution. At lower energy densities, the disorder in the effective field becomes binary, which leads to resonances not captured by our ansatz. We therefore start all sweeps of energy density at $\beta = 0.3$.

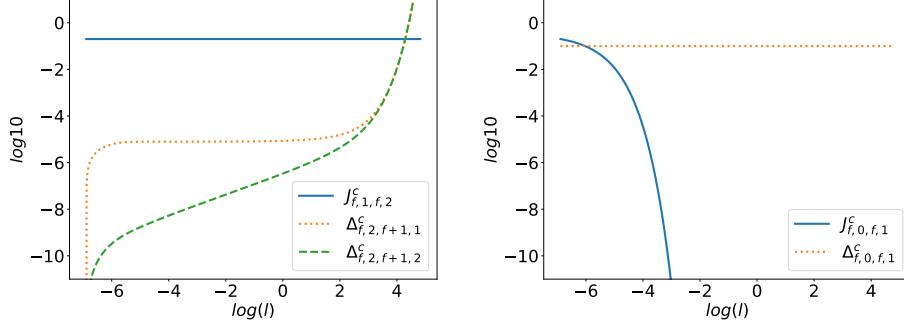


Figure S4: The flow of J_{ij}^c and Δ_{ij}^c for the geometry depicted in Fig. S5. The left panel shows the flow of couplings on the clean-chain sites that are not coupled to the dirty chain. It shows an unsuppressed hopping and diverging density-density coupling at long flow time l . The right panel shows the flow of couplings on the clean chain sites that involve a site that is coupled to the dirty chain. It shows that the hopping onto the coupled site, $r = 0$ (for any f), are suppressed and the density-density coupling involving a coupled site, remains constant.

equation ansatz can be avoided only by including the hoppings onto the coupled sites in the clean chain generator.

By choosing a disorder strength, W , in the dirty chain that is larger than the effective field strength, $\Delta < 2W$, we can ensure that the dirty chain has already transformed into the l-bit hamiltonian with $J_{ij}^d = 0$ at the flow time where hopping on the coupled sites in the clean chain is suppressed. The resulting $l = \infty$ hamiltonian will thus have no hopping in the dirty chain, no hopping on to the uncoupled sites, but with the sets of coupled sites communicating through the emergent next-nearest neighbour hopping across the coupled site: $J_{f,r=\delta-1,f'=f+1,r=1}(l = \infty)$. If this coupling was zero, the $l = \infty$ hamiltonian would have the set of integrals of motion depicted in Fig. S5: n_f^d , $n_{f,r=0}^c$ and $N_f = \sum_{r \neq 0} n_{f,r}^c$. Due to conservation of the second invariant, this coupling is necessary not zero, but it maybe smaller then the other couplings in $H(l = \infty)$ indicating that it is only important at long times.

By choosing the generator so that it only suppresses hopping onto the coupled site, we can make analytic estimates of the next-nearest neighbour hopping. To do so we first assume $\Delta \ll W$, so the flow of the dirty chain is done before there are significant changes to the clean chain. We can then treat the clean chain as a single chain with an effective field $\bar{h}_{f,r}$. We can then write the generator as:

$$\eta = \sum_f \eta_f \quad (\text{S26})$$

where:

$$\eta_f = -J\bar{h}_{f,r=0}J(c_{f-1,r=\delta-1}^\dagger c_{f,r=1} - c_{f,r=0}^\dagger c_{f,r=1} - h.c), \quad (\text{S27})$$

where J is the strength of the hopping on to the coupled site. Since $[\eta_f, \eta_{f'}] = 0$ for $\delta > 2$, we can focus on a single coupled site and its neighbours.

To do so and to simplify equations, we will label the coupled site as 0 and its left and right neighbours as -1 and $+1$. The above flow equations then dramatically simplify. The hopping and effective field couplings flow as:

$$\begin{aligned} \frac{d\bar{h}_{\pm 1}}{dl} &= -2J^2\bar{h}_0 \\ \frac{d\bar{h}_0}{dl} &= 2J^2\bar{h}_{+1} + 2J^2\bar{h}_{-1} \\ \frac{dJ}{dl} &= -J\bar{h}_0^2 \\ \frac{dJ_2}{dl} &= 2J^2\bar{h}_0, \end{aligned} \quad (\text{S28})$$

where J_2 is the magnitude of the next-nearest neighbour hopping, $J_2(l) = J_{f,r=\delta-1,f'=f+1,r=1}(l)$.

The flow of these couplings do not depend on the flow of the density-density coupling and can thus be solved independently. To do so, we use the assumption that $J \ll \bar{h}$ and note that the flow of J is much faster then the flow of the other couplings. Thus, assuming \bar{h} is constant we approximate the flow of $J(l)$ as:

$$J(l) = J(l=0)e^{-\bar{h}_0^2 l}. \quad (\text{S29})$$

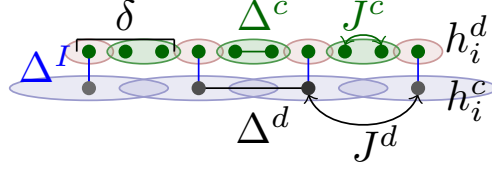


Figure S5: The portrait shows the dirty chain coupling to the clean chain every $\delta = 3$ sites. The emergent integrals of motion n_k^d (blue), $n_{f,r=0}^c$ (red) and N_f (green) are also depicted. This picture requires a sufficiently large Δ^I and $\langle n^d \rangle$, but does not require disorder in the effective field \bar{h}^c . When the clean-chain effective field is disordered, the remaining degrees of freedom contained in the uncoupled sites can localise.

again approximating \bar{h}_0 as constant we get

$$J_2(l) = -\frac{J^2}{\bar{h}_0} (1 - e^{-2\bar{h}_0^2 l}) \quad (\text{S30})$$

Thus, $\frac{\bar{h}_0}{J^2}$ is the characteristic time at which the integrals of motion, $n_{f,r=0}^c$ and N_f break down. A meaningful separation of time scales therefore requires $\bar{h}_0 \gg J^2$. In the following section, we discuss the form of this effective intermediate time hamiltonian.

Effective Hamiltonian at intermediate times

There are two possibilities for the intermediate time effective hamiltonian: 1) the density-density coupling between two neighbouring sets of uncoupled sites is smaller than J_2 or 2) it is larger. In the first case, this type of density-density coupling can be accurately dropped from the intermediate time effective hamiltonian. This leads to each set of uncoupled sites, labelled by f , evolving completely independently on intermediate times. This evolution can be thought of as the evolution of an effective spin of size:

$$|\vec{L}_f| = \frac{1}{2} \left(\frac{\delta - 1}{N_f} \right) + \frac{1}{2}. \quad (\text{S31})$$

The local map between the N_f fermions on $\delta - 1$ sites and the spin can be preformed by identifying the basis states labelled by the eigenvalues of $n_{f,r \neq 0}^c$ with the basis states labelled by the eigenvalues of L_f^z . Operators which are polynomial in the densities will then be mapped to operators which are polynomial in L_z . The remaining terms in the hamiltonian describe tunnelling within a set of uncoupled sites with all the same f . They describe transition between the L_f^z basis states and are thus described by polynomials in L_f^x and L_f^y .

For the second possibility, the local emergent spins will be coupled. Since the hopping operators at a site f commute with those at a site f' , a Jordan-Wigner string is not required to adjust statistics, and the coupled hamiltonian can be written as:

$$H(\{\bar{n}_f^d\}, \{\bar{n}_{f,r=0}^c\}, \{\bar{N}_f\}) = \sum_{ff'} F(L_f^z, L_{f'}^z) + \sum_f R_f(L_f^x, L_f^z, L_f^y), \quad (\text{S32})$$

where the function F depends on the intra-chain coupling, Δ^c and the function R depends on h^c , J^c , Δ^I , and Δ^c . In general, if the dirty chain or coupled sites have a disordered distribution of charges, the local operators, R_f , in the hamiltonian will be disordered. The question of whether the system is fully localized on intermediate times will then be dependent on any integrability present in this intermediate time hamiltonian or the extent to which R_f is disordered.

To determine which of the two cases is for the bare hamiltonian above, we compute the flow of $\Delta^c(k, k')$. We again focus on one coupled site, labelled by $r = 0$, and its neighbouring sites, labelled by $r = \pm 1$ (for any f). The flow equation equations for

the density-density couplings then becomes:

$$\begin{aligned}\frac{d\Delta_{-1,1}^c}{dl} &= 2J^2(\Delta_{-1,1}^c - \Delta_{0,1}^c) + 2J^2(\Delta_{-1,1}^c - \Delta_{0,-1}^c) \\ \frac{d\Delta_{0,1}^c}{dl} &= -2J^2(\Delta_{-1,1}^c - \Delta_{0,1}^c) \\ \frac{d\Delta_{-1,0}^c}{dl} &= -2J^2(\Delta_{-1,1}^c - \Delta_{0,-1}^c).\end{aligned}\tag{S33}$$

These coupled differential equations describe a rotation in a three-dimensional space at an instantaneous rate $2J(l)^2$. Given the assumption that $\Delta_{-1,1}(l=0) = 0$, this can be solved for the coupling between two sets of uncoupled sites as:

$$\Delta_{-1,1}(l) = \Delta_{0,1}(l=0) \left[1 - e^{\int_0^l dl' 2J^2(l')} \right]\tag{S34}$$

where:

$$\int_0^l dl' 2J^2(l') = \frac{J^2(l=0)}{\bar{h}_0^2(l=0)} (1 - e^{-2h_0^2 l})\tag{S35}$$

Therefore, the amplitude of the rotation in this three-dimensional space is small in J^2/\bar{h}_0^2 .

We are now in a place to discuss which of the above two possibilities is manifest in the hamiltonian discussed above. If $J_2(l=\infty) \ll \Delta_{-1,1}(l=\infty)$, then an interacting hamiltonian best describes the intermediate time dynamics while if the inequality is not satisfied a non interacting spin chain is the best description. Given the assumption $J \ll h$, this inequality simplifies to $h \ll \Delta$. Thus for the approximation made in ansatz hamiltonian above, we must take the case when $h > \Delta$ and conclude that the intermediate time hamiltonian describes a set of independently evolving spins.

Alternatively, we could assume the bare hamiltonian has a modest next-nearest neighbour coupling: $\Delta_{-1,1}(l=0) \approx \Delta_{0,1} < h$. In this case the rotation in Δ_{ij}^c space, described by Eq. S33, would still be of a small angle, but away from an initial vector with $\Delta_{-1,1}(l=0)$ already greater than $J_2(l=\infty)$. Intermediate time dynamics would then be described by a set of coupled emergent spins of size $|\vec{L}_f|$.

Explicit form of the Hamiltonian for $\delta = 3$

As an example, we now can consider $\delta = 3$ in which there are two uncoupled sites for each dirty site f and discuss the effective hamiltonian governing the intermediate time dynamics. The local Hilbert space for these two sites is 4 dimensional and the basis vectors can be labelled by the different ways in which 2 sites may be occupied with particles:

$$\{|00\rangle, |01\rangle, |10\rangle, |11\rangle\},\tag{S36}$$

where 1 indicates an occupied site. The local hamiltonian on these sites reflects the block diagonal structure enforced by the conserved charges:

$$\begin{bmatrix} 0 & 0 & 0 & 0 \\ 0 & \hat{\Delta}^L & J_{f2,f1}^c(l) & 0 \\ 0 & J_{f1,f2}^c(l) & \hat{\Delta}^R & 0 \\ 0 & 0 & 0 & \hat{\Delta}^{R+L} \end{bmatrix},\tag{S37}$$

where $\hat{\Delta}^L, \hat{\Delta}^R$, and $\hat{\Delta}^{R+L}$ are functions linear in the operators n_i^d and $n_{f' \neq f}^c$ and depend on the flow evolved intra and inter-chain couplings and fields h^c at flow time $l = \infty$. For $\delta = 3$ the conserved charge N_f has eigenvalues 0, 1, and 2 that correspond to the three blocks in Eq. S37. This block structure can be represented by two trivial spin-zero subspaces and one spin-half subspace.

We consider the case that $N_f = 1$ for each f , so that the local Hilbert space for the block of interest will be a spin-half. We can then perform the mapping to spin-halves via

$$\begin{aligned}L_f^z &= \frac{\hat{n}_{f,1} - \hat{n}_{f,2}}{2} \\ L_f^x &= \frac{c_{f,1}^\dagger c_{f,2} + h.c.}{2},\end{aligned}\tag{S38}$$

and the constraint $\frac{1}{2} = \frac{\hat{n}_{f,1} + \hat{n}_{f,2}}{2}$.

To apply this mapping, we write down the hamiltonian at the flow time $l = \infty$ as follows:

$$\begin{aligned} H &= \sum_f H_f + \sum_{f,f'} \sum_{r,r'=1,2} \Delta_{f,r,f',r'}^c n_{f,r}^c n_{f',r'}^c \\ H_f &= \sum_i \xi_{f,i} n_{f,i} + J_f^{un}(l) [c_{f,1}^\dagger c_{f,2} + c_{f,2}^\dagger c_{f,1}] \\ &\quad + \Delta_{f,1,f,2}^c n_{f,2}^c n_{f,1}^c, \end{aligned} \quad (\text{S39})$$

where $\xi_{f,i}$ is an effective field which depends on the bare fields at flow time l , the couplings Δ^c , Δ^I and the eigenvalues \bar{n}_f^d , $\bar{n}_{f,r=0}^c$ within the block of interest:

$$\xi_{f,i} = \bar{h}_{f,i}(l) + \sum_f \Delta_{f,i,f'}^I(l) \bar{n}_{f'}^d + \sum_f \Delta_{f,i,f',0}^c(l) \bar{n}_{f',0}^c.$$

Applying this mapping we get the spin hamiltonian:

$$H = \sum_f h_f^z L_f^z + h_f^x L_f^x + \sum_{ff'} \Omega_{f,f'} L_f^z L_{f'}^z + C \quad (\text{S40})$$

with

$$\begin{aligned} h_f^x &= 2J_f^{un}(l) \\ h_f^z &= \xi_{f,1} - \xi_{f,2} \\ \Omega_{f,f'} &= \Delta_{f,1,f',1}^C + \Delta_{f,2,f',2}^C - \Delta_{f,1,f',2}^C - \Delta_{f,2,f',1}^C. \end{aligned} \quad (\text{S41})$$

Here, we explicitly see how the spins are coupled by the next-nearest neighbour density-density couplings. Thus if the local spins are coupled at a strength less than the next-nearest neighbour hopping, $|\Omega_{f,f'}| < J_2$, the intermediate time dynamics describes independent spins rotating around an axis in the $x - z$ plane. While if $|\Omega_{f,f'}| > J_2$, then we have to consider the interacting spin problem to understand the intermediate time dynamics.

If there is no disorder in the dirty and coupled site charge distributions, the z component of the local field, h_f^z will be null and the translationally-invariant emergent spin-model will be a transverse field Ising model. This hamiltonian is integrable via the Jordan-Wigner transformation:

$$\begin{aligned} L_f^x &\rightarrow n_f^a - 1/2 \\ L_f^z L_{f'}^z &\rightarrow (a_j^\dagger - a_j)(a_{j+1} + a_{j+1}^\dagger), \end{aligned} \quad (\text{S42})$$

which produces a single particle hamiltonian in the Jordan-Wigner fermions. Thus the model will realize an interesting possibility where, on intermediate time scales, the system is non-ergodic where local-in-real-space blocks of magnetization are conserved (recall that N_f is conserved), and local-in-momentum-space integrals of motion (the diagonal Jordan-Wigner fermion densities) are as well conserved.

If the dirty and uncoupled sites are disordered, the h_f^z field will lead to terms which break integrability and thermalize the emergent spins. Thermalization would then take place in two stages. In the first, the effective spins thermalize with respect to the intermediate time hamiltonian. While in the second stage, the system thermalizes to full hamiltonian in which the charges N_f are no longer conserved.

While if the disorder field, h_f^z , dominates over the transverse field, h_f^x , the emergent spin chain will again become fully non-ergodic on intermediate time scales, but with a complete set of local integrals of motion. We have confirmed these expectations via exact diagonalization of the intermediate time hamiltonian with a comparison of the level spacing statistics to a Wigner-Dyson or Poisson distribution. In this calculation, the number of dirty sites is $N_s = 8$ and the number of dirty sites is $\delta N_s = 24$. Thus, the initial unitary computed by the flow equation is necessary to perform an exact diagonalization because a 32 site spin chain would be hardly practicable via exact diagonalization.

NUMERICAL DETAILS

The flow equations are numerically solved using an adaptive step 4^{th} order Runge-Kutta. We work with a clean chain length of 24 sites $\delta N_s = 24$ for a total of 48 sites (32 sites when $\delta = 3$). We control the adaptive step by attempting around 800 discrete Runge-Kutta steps on a log scale from $l = 10^{-3}$ to $l = 10^2$. The adaptive step usually requires additional steps to reach the desired accuracy result in an average number of steps of around 3000

Since our results requires an accuracy for the couplings on a scale absolute scale 10^{-20} , we devoted careful attention to numerical errors. We found that numerical errors were due floating point errors for numbers close to 0 during the first step and at latter times. Numerical errors in the first step of a Runge-Kutta approximation are well know, while the ones at later times are due to the form of the flow equations. These long time error are due to contributions like $\sum_k J_{ik} J_{kj} (h_i + h_j - h_k)$ that could easily flip sign and cause numerical noise at longer times during the flow.

To manage these errors, we initialized the hoppings J_{ij} for $i \neq j \pm 1$ to ϵ_1 and treated a hopping with $|J_{ij}| < \epsilon_2$ as exactly 0. This fixed the numerical errors when $\epsilon_2 > 10^{-15}$ and $\epsilon_1 > \epsilon_2$. Since J_{ij} contributes to the flow of Δ_{ij} at second order, this approximation leads to an error in Δ_{ij} less than ϵ_2^2 . We tested the validity of these numerical approximations by varying ϵ_1 and ϵ_2 and observing no change in the flow.